EPJ Photovoltaics **14**, 17 (2023)

https://doi.org/10.1051/epjpv/2023008

Available online at:
www.epj-pv.org

REGULAR ARTICLE OPEN ACCESS

# Reverse-bias behaviour of thin-film solar cells: effects of measurement-induced heating

Stephan J. Heise[1,*], Asliddin Komilov[2], Michael Richter[1], Bart Pieters[3], Andreas Gerber[3] and Janet Neerken[1]

[1] Ultrafast Nanoscale Dynamics, Institute of Physics, University of Oldenburg, 26111 Oldenburg, Germany
[2] Physical-Technical Institute of the Academy of Sciences of the Republic of Uzbekistan, Chingiz Aitmatov 2B, 100084 Tashkent, Uzbekistan
[3] IEK5-Photovoltaik, Forschungszentrum Jülich, 52425 Jülich, Germany

Received: 5 January 2023 / Received in final form: 24 February 2023 / Accepted: 27 February 2023

**Abstract.** When a solar cell is subjected to a negative voltage bias, it locally heats up due to the deposited electrical power. Therefore, every investigation of cell characteristics in the negative voltage regime faces the challenge that the measurement itself changes the state of the cell in a way that is difficult to quantify: On the one hand, the reverse breakdown is known to be strongly temperature dependent. On the other hand, negative voltages lead to metastable device changes which are also very sensitive to temperature. In the current study, we introduce a new approach to suppress this measurement-induced heating by inserting time delays between individual voltage pulses when measuring. As a sample system we use thin-film solar cells based on Cu(In,Ga)$Se_2$ (CIGS) absorber layers. First we verify that with this approach the measurement-induced heating is largely reduced. This allows us to then analyse the impact of the heating on two characteristics of the cells: (i) the reverse breakdown behaviour and (ii) reverse-bias-induced metastable device changes. The results show that minimising the measurement-induced heating leads to a significant increase of the breakdown voltage and effectively slows down the metastable dynamics. Regarding the reverse breakdown, the fundamental tunneling mechanisms that are believed to drive the breakdown remain qualitatively unchanged, but the heating affects the quantitative values extracted for the associated energy barriers. Regarding the reverse-bias metastability, the experimental data reveal that there are two responsible mechanisms that react differently to the heating: Apart from a charge redistribution at the front interface due to the amphoteric ($V_{Se}$–$V_{Cu}$) divacancy complex, the modification of a transport barrier is observed which might be caused by ion migration towards the back interface. The findings in this study demonstrate that local sample heating due to reverse-bias measurements can have a notable impact on device behaviour which needs to be kept in mind when developing models of the underlying physical processes.

**Keywords:** Reverse breakdown / partial shading / metastability

## 1 Introduction

The reverse current–voltage ($I$–$V$) characteristics of solar cells become relevant in situations where an array of cells that are connected in series—e.g. a photovoltaic module—is partially shaded. In that case any shaded cell "sees" the cumulative photovoltage of all other cells, so that the blocking behaviour of that cell may break down and allow for current flow. The amount of electric power that is then deposited as heat in the shaded cell equals the product of current and voltage and therefore critically depends on the reverse IV characteristics: If the breakdown voltage is large (highly negative), breakdown sites may heat up to several hundred degrees centigrade which will result in permanent damage [1–4]. However, if the breakdown voltage is low, operation is less critical and the cell may act as an internal bypass. In monolithically integrated module designs, which are standard in thin film technology, external bypass diodes are inherently difficult to integrate and, hence, manufacturers usually rely on the internal bypass and accordingly target low breakdown voltages.

Therefore, it is important to thoroughly understand the mechanisms that govern the reverse breakdown in thin-film solar cells. However, when developing physical models, the interpretation of the reverse IV characteristics is complicated by the fact that the cell actually heats up during the experiment due to the deposited electric power. That is, on the one hand the cell temperature cannot be assumed to be constant during a reverse IV measurement. But on the

* e-mail: Stephan.Heise@uni-oldenburg.de

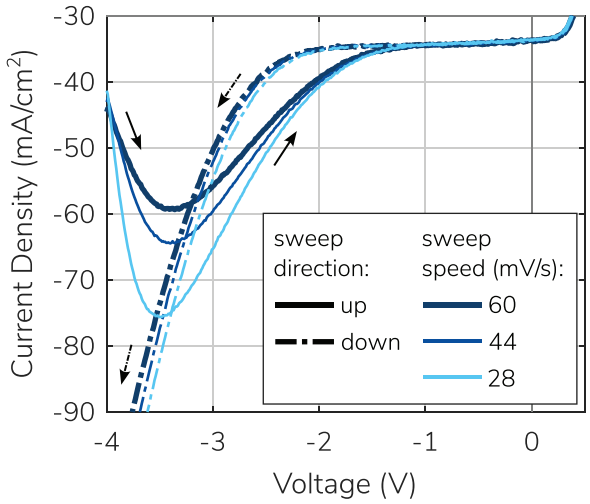


**Fig. 1.** Hysteresis in reverse IV measurements. Up-sweeps with increasing voltage (solid lines) lead to different results than down-sweeps with decreasing voltage (dashed-dotted lines). The reverse IV curve is also influenced by the speed of the voltage sweeps (colour-coded).

other hand the breakdown behaviour is known to be extremely temperature dependent [5,6]: With increasing temperature, the breakdown voltage shifts towards lower (absolute) values. This issue poses a challenge for developing appropriate quantitative models of the reverse breakdown.

In solar cells based on chalcopyrite $Cu(In,Ga)Se_2$ (CIGS) absorbers, the temperature-dependence of the breakdown behaviour is nicely demonstrated by the hysteresis that is observed when measuring the reverse IV curve either with increasing or decreasing voltage sweeps (Fig. 1). When starting the measurement at positive voltages (down-sweep), the deposited power gradually increases with increasing negative voltage and the sample heats up continuously, which results in a monotonic IV curve. When starting the measurement at negative voltages (up-sweep), however, the sample is at ambient temperature initially where the blocking behaviour is good and current flow is low, but then it heats up very rapidly due to the high electric power, so that the current increases significantly until the temperature reaches a maximum and then decreases. As can be seen from Figure 1, this effect depends on the speed of the voltage sweeps which supports the claim of its thermal origin.

Apart from heating the material, a further effect of the negative voltage applied during the reverse IV measurement may be a metastable change of the device characteristics. In CIGS devices, for instance, the application of a reverse voltage is known to reduce the fill factor FF [7–10] and the open-circuit voltage $V_{OC}$ [11,12]. This is commonly explained by the ($V_{Se}$–$V_{Cu}$) divacancy complex which can change from an acceptor- to a donor-configuration under reverse bias [13]. Although this effect is less influential on the reverse IV curve than the electrical heating, small changes in FF and $V_{OC}$ due to reverse IV measurements are typically observed. Moreover, the metastable acceptor–donor conversion itself is temperature dependent [14], so that the measurement-induced heating may actually distort the resulting IV curve in *two* ways.

In this study we aim at generating temperature-stable reverse IV curves by introducing pauses in the voltage sweeps. Although this approach does not evaluate the cell's reverse behaviour under realistic operation conditions, it allows us to identify the role of temperature for the reverse breakdown and to test our understanding of the breakdown physics. After verifying that measurement-induced heating is indeed largely suppressed by introducing the pauses, we compare the results to conventionally measured breakdown characteristics in order to quantitatively estimate both the amount of heating as well as the consequences of heating-induced distortions on the interpretation of the underlying breakdown mechanisms. Further, we investigate how the measurement-induced heating affects reverse-bias-induced metastable device changes and examine their impact on the reverse IV characteristics.

## 2 Methods

### 2.1 Experimental details

The samples used in this study were provided by the NICE Solar Energy GmbH and had the typical layer stack of Mo/$Cu(In,Ga)Se_2$/CdS/i-ZnO/ZnO:Al on a glass substrate, where the CIGS absorber layer was deposited via coevaporation. Lab-scale samples were cut from two batches of full-size modules (with cell efficiencies in the range of 13% and 16%, respectively). The samples in the first part of the paper (batch #1) had an active area of about 1 $cm^2$ and were contacted with gold needles via metal grid fingers on top of the ZnO layer. The samples of the metastability experiments (batch #2) were sized $0.5 \times 0.5\,cm^2$ and were contacted directly on the ZnO layer. The Mo back electrode was contacted outside the active cell area. In all cases illuminated lock-in thermography images (from a Thermosensorik setup) ensured that only material without localised hotspots was selected.

Room-temperature IV measurements were obtained in a AAA solar simulator (PET SS100AAA). For illuminated measurements the lamp intensity was adjusted to 1000 $W/m^2$ with a calibrated Si reference cell. During the measurements the samples were kept at 25 °C with the help of a water-heated sample stage.

Temperature-dependent IV measurements from 300 K down to 220 K were performed in a closed-cycle helium contact gas cryostat (CryoVac) with a LakeShore 336 temperature controller. Illumination was provided by a Xenon lamp whose light passed through a water filter. The intensity was calibrated such that the short-circuit current of the device under test matched its short-circuit current measured at standard test conditions in the room-temperature setup.

In both IV setups, a Keithley 2400 sourcemeter was used to apply voltages and measure currents in a four-point-probe configuration. The settings differed between standard and reverse IV measurements: In order to minimize sample heating during the application of reverse voltages, these measurements were performed rather

quickly by recording only a single current reading per voltage. Therefore these data are somewhat noisier than the standard voltage sweeps (average over three current readings).

Capacitance-voltage (CV) profiles were obtained in the dark at a frequency of 50 kHz and an AC oscillation amplitude of 30 mV using a Solartron 1260A impedance analyser. For the Mott-Schottky analysis a $C_p$–$R_p$ equivalent circuit and a dielectric constant of $\varepsilon_{\mathrm{CIGS}} = 13$ were assumed.

For investigating the reverse-bias metastability, the order of the measurements was as follows: IV, CV, reverse-bias treatment, CV, IV. The reverse-bias treatment consisted of applying −5 V for a variable amount of time. All measurements were done in the dark without illumination. Every cell was treated only once in order to ensure a comparable initial state of the cells.

## 2.2 Intermittent voltage sweeps

In order to assess the effects of sample heating during the measurement, the voltage was either applied continuously (as usual) or with breaks between the individual voltage pulses. A sketch of the two types of voltage signals—which will be referred to as *continuous* (CONT) and *intermittent* (INT) in the following—is shown in Figure 2a.

In order to compare the amount of measurement-induced sample heating for the two approaches, as a first test we monitored the current while applying a constant negative voltage of −3 V. The results are shown in Figure 2b. Note, that here the horizontal axis shows the "on"-time in which a voltage was applied. For the continuous measurement this corresponds to the actual measurement time, but for the intermittent case the actual measurement duration corresponding to 60 s "on"-time was about 6.5 min. The results show a striking difference between the two cases: The continuously applied voltage leads to a steady increase of the current during the measurement, which we attribute to electric sample heating and which closely resembles the evolution of the shunt temperature in electro-thermal simulations reported by Guthrey et al. [4][1]. For the intermittent voltage application, in contrast, the current stays more or less constant throughout the measurement. This indicates that the voltage pause in the intermittent case is long enough, so that any heating induced by the previous voltage pulse can relax before the next measurement pulse is applied.

As a second test we compared reverse IV characteristics for continuous and intermittent voltage sweeps by making use of the fact that, before any voltage sweep, the sample is in thermal equilibrium, so that the first few data points of a measurement should not be affected by measurement-induced heating (this could already be observed in the up-sweeps in Fig. 1). Therefore, we performed a set of continuous sweeps from low to high voltages with a variation of the starting voltage. Here, the voltage sweeps

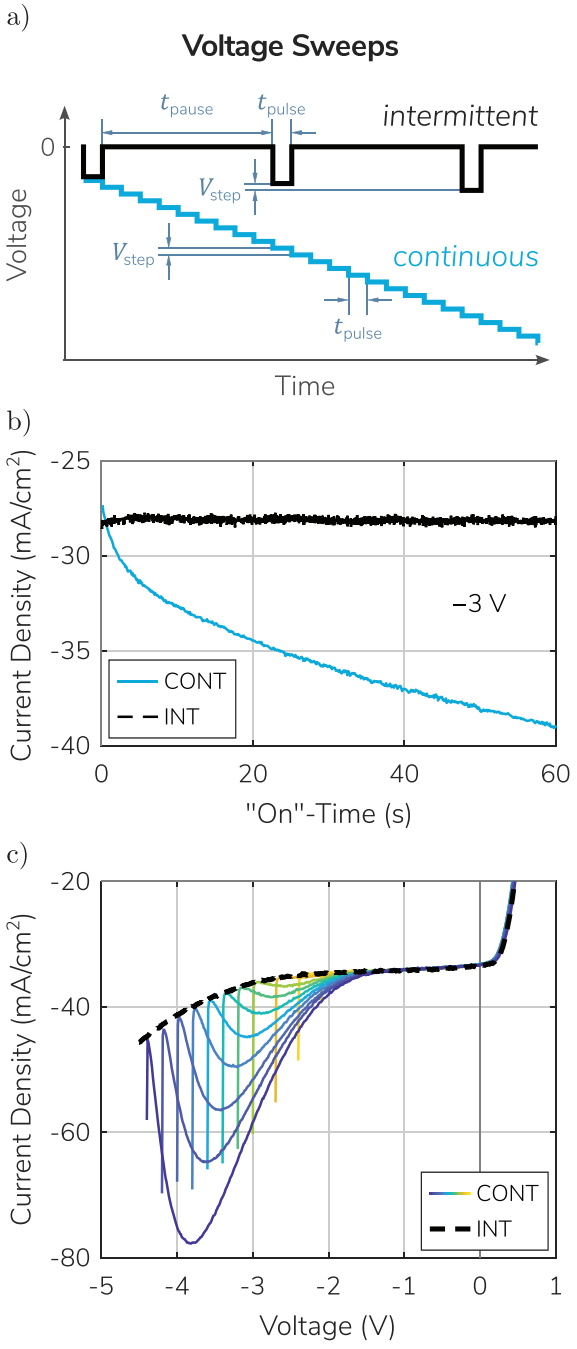


**Fig. 2.** Suppressing sample heating with intermittent voltage sweeps. (a) Sketch of the two types of voltage sweeps. (b) Evolution of the current density upon application of a constant reverse voltage of −3 V under illumination of one sun (INT with $t_{\mathrm{pause}} = 1.5$ s). (c) Continuously swept reverse-IV measurements (up-sweeps) starting from different voltages (solid coloured lines) in comparison with an intermittently swept measurement (dashed black line, $t_{\mathrm{pause}} = 1.0$ s).

were applied with our standard (slow) parameters. The results in Figure 2c (solid lines) show that after the first 1–2 data points a peak in the current is reached that should reflect the "true" IV characteristics at this point (the behaviour of the very first points is assumed to be a

[1] The fact that the current does not increase exponentially here shows that the self-amplifying feedback loop of temperature and current gains is damped by some mechanism, for instance by thermal conduction away from the local breakthrough sites.

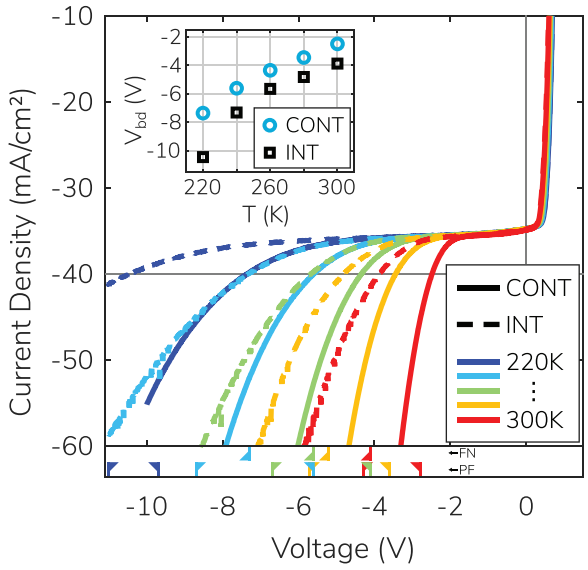


**Fig. 3.** Temperature-dependent breakdown behaviour for continuous (solid lines) and intermittent (dashed lines) voltage sweeps. The coloured arrows at the bottom indicate the limits of the linear regions of the INT data in the Fowler-Nordheim (FN) and Poole-Frenkel (PF) plots (only lower limit for FN). Inset: Breakdown voltage as $V(-40\,\mathrm{mA/cm^2})$ as a function of temperature.

measurement artefact which occurs when the delay time between voltage application and current measurement is too small). So by using different starting voltages, step by step a reverse IV curve can be constructed which is not distorted by measurement-induced heating. As Figure 2c reveals, this constructed IV curve seems to coincide with the IV curve obtained by using an intermittent voltage sweep (dashed line). This coincidence is a further indication that measurement-induced sample heating is suppressed when using intermittent voltage sweeps. Of course, the suppression of measurement-induced heating will become less complete, if we go to even higher negative voltages or reduce the interval $t_{\mathrm{pause}}$ between the voltage pulses.

## 3 How does heating affect the reverse breakdown?

Now we use the intermittent voltage sweeps to investigate the measurement-induced heating in more detail and to check if our understanding of the breakdown mechanisms in CIGS changes when we analyse IV characteristics that are not distorted by heating effects. To this end, we performed temperature-dependent IV measurements under illumination for continuous and intermittent voltage sweeps ($V_{\mathrm{step}} = 10$ mV, $t_{\mathrm{pause}} = 1.0$ s, $t_{\mathrm{pulse}} = 20$ ms) from room temperature down to 220 K, when the sample died during the measurement (irreversible breakdown). The results are given in Figure 3, which also shows the temperature-dependent breakdown voltage as an inset. Here, the breakdown voltage was defined as the voltage at which the IV curve reached $-40$ mA/cm$^2$ (these values are virtually identical to the values of $V_{\mathrm{br}}$ as defined by Puttnins et al. [15], but better extractable).

As a first result, we observe that the breakdown for the continuous sweeps is strongly shifted to lower (negative) voltages compared to the breakdown for intermittent sweeps. This shift is also clearly visible in the breakdown voltages in the inset of Figure 3. By comparing the curves we can estimate the magnitude of the measurement-induced heating for the continuous sweeps: At ambient temperatures of 220 K and 240 K the continuously measured IV curves almost perfectly coincide with the intermittently measured data at 240 K and 260 K ambient temperature, respectively. In other words, here the continuous sweeps led to a heating of the breakdown sites of 20 K. This is at least twice as much as one would expect from a simple one-dimensional heat conduction model[2], thus supporting the idea that the temperature distribution in the cell is non-uniform and breakdown sites are very localized. The heating seems to increase towards higher temperatures: For the 260 K continuous measurement the temperature increase is around 30 K. This is probably caused by the non-linear temperature-dependence of the responsible tunneling currents. However, it cannot be excluded that the longer light-soaking during the intermittent measurements also has some effect (metastable changes due to the negative voltages are unlikely to play a role, see Sect. 4).

Regarding the mechanisms governing the reverse breakdown, the similarity of the shapes of the breakdown characteristics for continuous and intermittent voltage sweeps suggests that, in general, the fundamental mechanisms driving the breakdown in the two cases are the same. However, the deviations at higher (negative) currents indicate that differences in the details of the breakdown do exist.

The data in Figure 3 show that the breakdown voltage has a negative temperature coefficient, i.e. towards higher temperatures the breakdown shifts to lower (absolute) voltages. This is true for both kinds of voltage sweeps and also for lower intensities including the dark (not shown). Between 260 K and 300 K this shift is linear with a slope of $-45$ mV/K. In accordance with literature data [5,15], the sign and the magnitude of the temperature coefficient give strong evidence against impact ionization (Avalanche breakdown) as being responsible for the breakdown in CIGS.

Instead, the reverse breakdown in CIGS solar cells is believed to be mainly driven by two tunneling mechanisms [6,16]: (i) tunneling through a triangular barrier at the CIGS/CdS heterointerface (conduction-band spike), which can be described by the Fowler-Nordheim model [17].

[2] According to Fourier's law, $\Delta T = P \cdot d/k$, the temperature difference between the front and the back side of the glass (which provides an upper limit for the temperature difference between the continuous and the intermittent case) should be around 10 K, if we assume Joule heating of $P = -7\mathrm{V} \cdot (-50)\,\mathrm{mA/cm^2}$ and a $d = 3$ mm thick glass with a conductivity of $k = 1\mathrm{W/(Km)}$.

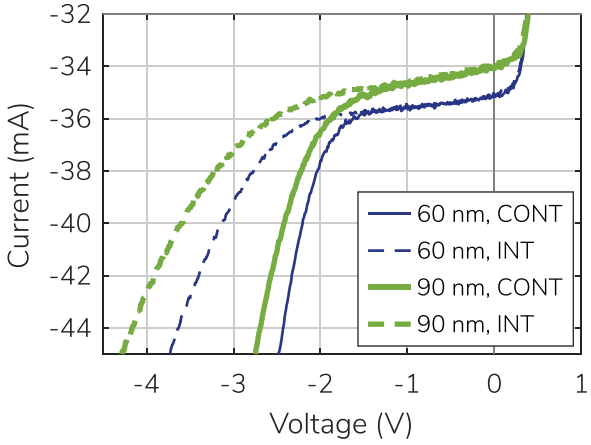


**Fig. 4.** Reverse IV characteristics for samples with two different thicknesses of the CdS buffer layer for continuous (solid lines) and intermittent (dashed lines) voltage sweeps. Average data of three samples per thickness are shown.

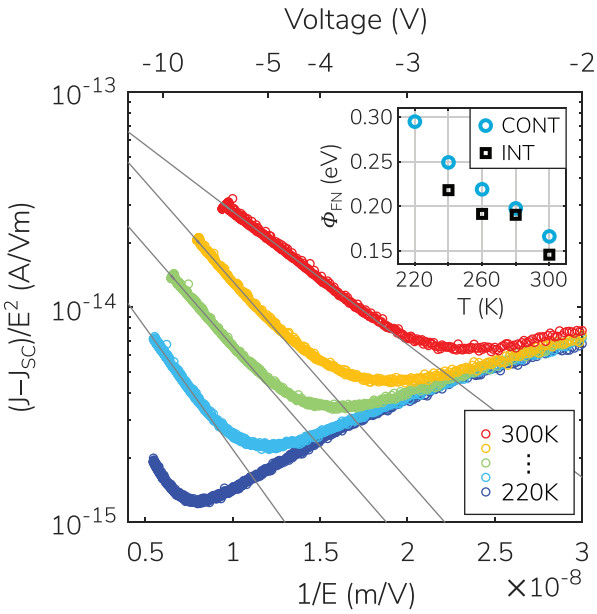


**Fig. 5.** Fowler-Nordheim analysis of the temperature-dependent IV characteristics measured with intermittent voltage sweeps that were shown in Figure 3. The lines show linear fits to the experimental data (coloured circles). The inset shows the Fowler-Nordheim barrier $\Phi_{FN}$ extracted from the linear fits for both continuously and intermittently measured data.

(ii) Tunneling via defect states in the band gap, which can be described by the Poole-Frenkel model [18]. Both models predict an increase of tunneling currents with increasing temperature, which agrees with the observed decrease in breakdown voltage. Further, it has been shown that the voltage drop in the CdS buffer layer plays a crucial role for the breakdown [5,16,19,20]. So far, these models have only been tested on IV characteristics measured with continuous voltage sweeps, so that heating effects may have led to misinterpretations. Therefore, next we analyse how the usage of intermittently measured IV characteristics might change our understanding of the reverse breakdown.

We start by examining the role of the CdS buffer layer and compare the breakdown characteristics of samples in which the thickness of the buffer layer was modified by changing the duration of the chemical bath deposition. Figure 4 shows that the breakdown voltage increases with increasing buffer layer thickness regardless of whether we use continuous or intermittent voltages sweeps for the measurement. This clearly shows that this effect is not an artifact due to measurement-induced sample heating, and it substantiates previous conclusions that the voltage drop in the CdS layer is essential for the reverse breakdown.

Next, we analyse the tunneling processes. The Fowler-Nordheim tunneling current may be expressed as [21]

$$J_{FN} = C_{FN}\frac{q^3E^2}{8\pi h\Phi_{FN}}\frac{m_{\mathrm{CIGS}}}{m_{\mathrm{CdS}}}\exp\left(-\frac{8\pi\sqrt{2m_{\mathrm{CdS}}\Phi_{FN}^3}}{3qhE}\right) \quad (1)$$

where $\Phi_{FN}$ is the height of the barrier, $E$ is the electric field which contains information about the width of the barrier, and $C_{FN}$ is a scaling factor which was introduced by Bakker et al. [6] to fit their experimental data. (Further, $q$ is the electric charge, $h$ Planck's constant and $m_i$ the effective electron mass in material $i$.) According to equation (1), a semilogarithmic plot of $(J-J_{\mathrm{SC}})/E^2$ versus $1/E$ should be linear if Fowler-Nordheim currents dominate. Figure 5 shows the Fowler-Nordheim plot of the intermittently measured IV characteristics for different temperatures. Here, the common assumption was made, that the applied voltage $V_{\mathrm{app}}$ drops entirely over the buffer layer for all $T$, so that the electric field may be calculated as $E = V_{\mathrm{app}}/d_{\mathrm{CdS}}$ (with $d_{\mathrm{CdS}}$ the thickness of the buffer layer) [6,16,20]. The data clearly show a linear behaviour above a certain voltage (for 220 K this voltage apparently exceeded the measured range). This indicates that Fowler-Nordheim tunneling dominates the reverse breakdown at higher (negative) voltages which is in agreement with previous reports [6,16].

By using equation (1), the barrier height $\Phi_{FN}$ may be extracted from the slope of the linear region in the Fowler-Nordheim plot [22]. The inset of Figure 5 shows the corresponding temperature-dependent barriers (black squares) in comparison with the barriers extracted from the continuously measured data (blue circles). For this purpose $m_{\mathrm{CIGS}} = 0.09m_e$ and $m_{\mathrm{CdS}} = 0.14m_e$ (with $m_e$ the free electron mass) were used [23]. Fowler-Nordheim tunneling barrier heights seem to be in the range of a few hundred meV and decrease with increasing temperature. However, the measurement-induced heating in the continuous voltage sweeps seems to lead to an increase of the extracted barrier height values of approximately 14%. Further differences between the continuously and intermittently measured data are observed in the scaling factor $C_{FN}$ which is about an order of magnitude higher ($10^{-7}$ vs. $10^{-8}$) and has a 80-meV higher activation energy (180 vs. 100 meV) for the continuous sweeps than for the intermittent sweeps.

In a similar manner, the data may be analysed for Poole-Frenkel tunneling. Linear regions in a semilogarithmic plot of $(J-J_{SC})/E$ versus $\sqrt{E}$ indicate that defect-assisted Poole-Frenkel tunneling is the dominant contribution to the breakdown current [16]. For the intermittently measured data the linear regions of the Poole-Frenkel plot are indicated at the bottom of Figure 3. If we compare them to the Fowler-Nordheim regimes, it becomes clear that the Poole-Frenkel mechanism seems to dominate at lower (negative) voltages before the Fowler-Nordheim mechanism takes over at higher voltages. The extraction of the Poole-Frenkel barrier height $\Phi_{PF}$ from the slope of a linear fit in the Poole-Frenkel plot is much less accurate than in the above case of $\Phi_{FN}$ because in this voltage region also further sources contribute to the total current in a non-negligible way (for a more reliable extraction, a complete model of the reverse current as has been used elsewhere [6,16] would be needed). However, qualitatively the analysis indicates that the Poole-Frenkel barrier height extracted from the continuous voltage sweeps is some tens of meV lower than $\Phi_{PF}$ extracted from the intermittent voltage sweeps. In other words, the barrier height $\Phi_{PF}$—which is equivalent to the ionization energy of the defect level that participates in the tunneling process—is probably underestimated, if it is derived from continuous measurements, in which heating was not suppressed.

At even lower (absolute) voltages in the pre-breakdown regime, the IV data for continuous and intermittent voltage sweeps are very similar. In contrast to other studies [6,24,25] we do not find any hints for significant space-charge limited currents (SCLC) in this regime in our cells. SCLC are characterised by a power-law IV relation with an exponent of 2 or larger. However, in our data the slope of the double-logarithmic IV plot (not shown) is approximately 1 at 0 V, and then slowly decreases towards more negative voltages until the Poole-Frenkel regime sets in.

In conclusion, the comparison of the breakdown characteristics including and excluding measurement-induced heating showed that the basic mechanisms of the reverse breakdown under illumination are the same: The onset of breakdown is governed by Poole-Frenkel tunneling currents, whereas the Fowler-Nordheim tunneling mechanism dominates at higher voltages. However, quantitative differences are notable: Measurement-induced heating leads to a significant reduction of the breakdown voltage (≈1.4 V at room temperature), an overestimation of the Fowler-Nordheim barrier height (≈14%), and an underestimation of the Poole-Frenkel barrier height. This should be kept in mind when modelling the reverse breakdown in CIGS.

## 4 How does heating affect the reverse-bias metastability?

It has been known for a long time that applying a negative voltage induces metastable changes in CIGS devices [26–29]. Here, we use the paradigm of continuous and intermittent voltage application to investigate the effect of measurement-induced heating on the dynamics of the reverse-bias metastability in the dark. The objective is twofold: On the one hand, we expect that the new approach can help to advance our understanding of the mechanisms that drive the metastable changes. On the other hand, we want to assess the influence of the reverse-bias metastability on the measurement of the reverse breakdown behaviour.

For this purpose, we applied a negative bias voltage of $V_R = -5$ V in the dark for varying durations either continuously or intermittently ($t_{\text{pause}} = 1.5$ s, $t_{\text{pulse}} = 100$ ms), and analysed the effect of this treatment on the IV and CV characteristics. The results are shown in Figure 6.

The IV measurements in panel a) show that the reverse-bias treatment leads to a noticeable shift of the IV curve in the injection regime that increases the longer the treatment lasts. To quantify this shift, the change of the voltage at a fixed current density of 90 mA/cm$^2$ is plotted as a function of the duration of the $V_R$ treatment in panel b). The data show a steady increase of the shift with $V_R$ duration, which is slightly smaller for the intermittent treatment than for the continuous treatment. This indicates that the process responsible for the shift is mildly temperature-activated.

The results of the CV measurements show that also the capacitance (panel c) and the doping density (panel d) are significantly affected by the reverse-bias treatment. However, in contrast to the IV shift, here the changes are not monotonic for the continuous treatment: First the capacitance and the doping density increase with increasing duration of the treatment, but for very long durations, both parameters drop again. The effects of the intermittent $V_R$ treatments tend to be much smaller than for the continuous treatments. It should be noted, that the effects on the CV characteristics are systematically slightly underestimated here, because of a metastable capacitance change induced by the IV measurement[3]. This also explains the apparent doping *reduction* seen for the intermittently treated data.

Based on these results, we now try to disentangle the different mechanisms that contribute to the reverse-bias metastability. The increase in doping density and capacitance under reverse bias is commonly explained by the Lany-Zunger model [14] in terms of the amphoteric nature of the ($V_{\text{Se}}$–$V_{\text{Cu}}$) divacancy complex: Depending on the Fermi level, this complex can exist in a donor or in an acceptor configuration. In equilibrium, the divacancy complex acts as a compensating donor in the bulk of the absorber layer, and as an acceptor towards the front interface. Under reverse-bias the Fermi level is shifted so that a donor-to-acceptor transition can take place in the space-charge region, which leads to an increased net doping

[3] This IV-induced change is of the order of $\lesssim +2$ nF (equivalent to 50 nm narrowing of the space-charge region) and a factor of $\lesssim$1.4 in $N_A$, and relaxes within about 15 min. In the measurement protocol a period of 5 min was introduced between the initial IV and CV measurements (measurement order: IV, Cf, CV, $V_R$, CV, IV) in order to reduce this effect, but nevertheless the initial CV measurement was slightly affected by the relaxation of the IV-induced changes, so that the $V_R$-induced capacitance and doping changes in Figure 6c+d are slightly underestimated.

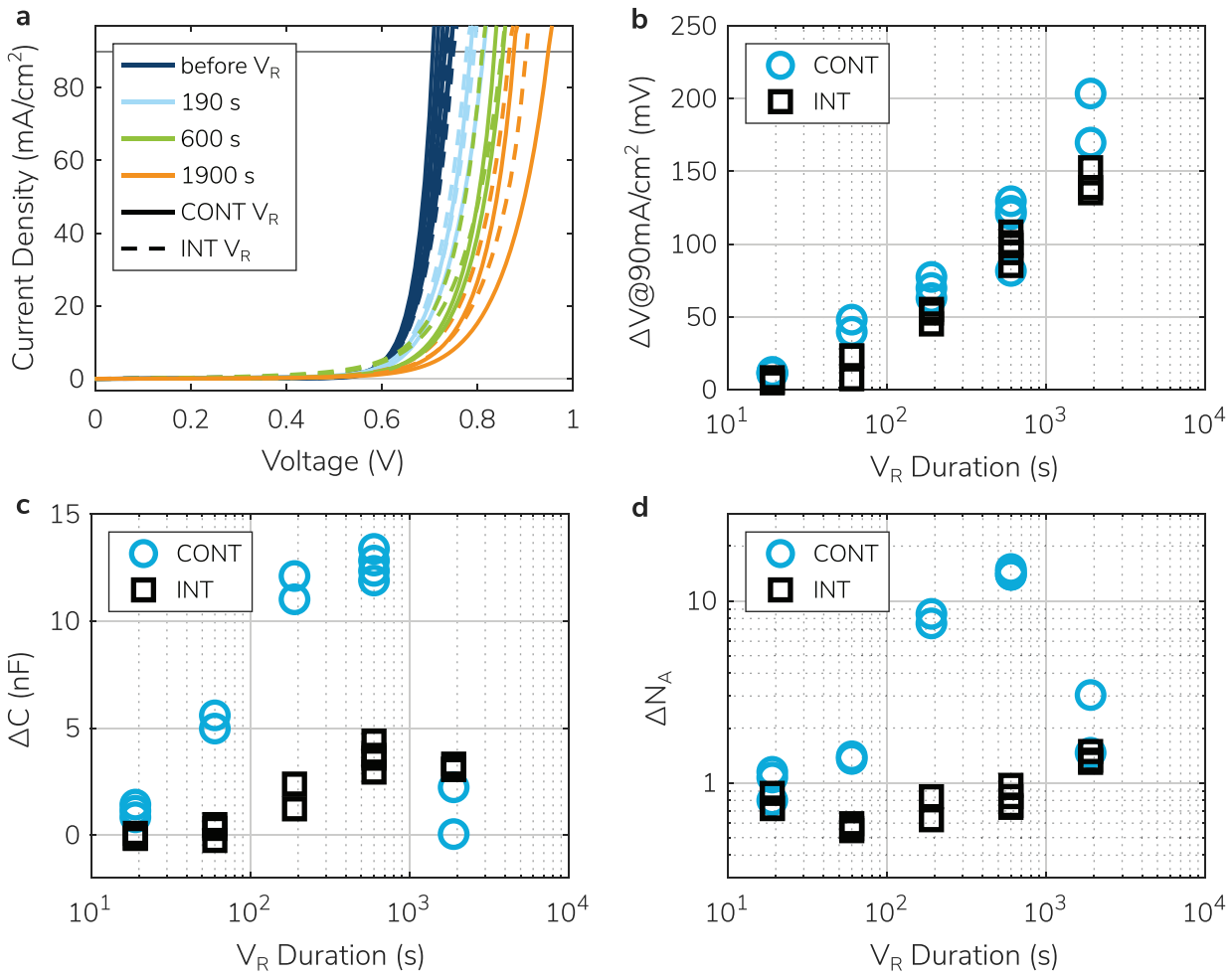


**Fig. 6.** Metastable changes due to reverse-bias ($V_R$) treatments in the dark (2–4 samples per condition). (a) IV characteristics before (dark blue) and after continuous (solid lines) and intermittent (dashed lines) $V_R$ treatments of different durations (colour-coded). (b) Shift of the voltage at 90 mA/cm$^2$ (see grey line in a), (c) shift in capacitance at 0 V, and (d) shift in doping density (ratio: $\Delta N_A := N_A^{\text{after}}/N_A^{\text{before}}$) after reverse-bias treatments of different durations ("on"-time) and different modes (continuous: circles, intermittent: squares).

density. This transition is coupled to an energy barrier of approximately 0.7 eV. Without bias the system can relax via the acceptor-to-donor transition, which includes an energy barrier of approximately 0.3 eV and requires two free holes.

This model is able to nicely explain our results in Figure 6c+d for $V_R$ durations up to 190 s. The metastable changes are larger for the continuous $V_R$ treatments than for the intermittent treatments because the measurement-induced heating provides additional energy to overcome the barrier $\Delta E$ associated with the donor-to-acceptor transition. Assuming that the transition rate follows $\tau^{-1} \propto \exp(-\Delta E/kT)$, we can estimate the temperature difference between the continuous and intermittent 190-s-treatments to be 18 K, which is quite consistent with what we derived from the temperature-dependent measurements in Figure 3.

For longer $V_R$ durations a second mechanism seems to start to dominate the CV results, which eventually counterbalances the charge redistributions caused by the divacancy complex. A similar behaviour has been reported by Urbaniak & Igalson [30,31] who coupled the drop in capacitance to an interface barrier seen in the double-diode characteristics of the illuminated IV curve. Also the shift of our IV data in Figure 6a indicates the increase of an interface barrier: The shift is observed in the diode current (and not due to the shunt current as in the samples of Dongaonkar et al. [32]), mainly as an increase of a non-linear series-resistance-like contribution. It has been proposed that such a barrier could form in the conduction band of the absorber layer close to the front interface due to the increased amount of positive charges caused by the donor-to-acceptor transition of the divacancy complex under reverse bias ("$p^+$ layer") [11,33]. However, the differences between continuous and intermittent $V_R$ treatments seem to be much smaller for the IV shift (Fig. 6b) than for the capacitance and doping shifts (Fig. 6c+d). Therefore it seems questionable that the increase of the barrier is directly coupled to the changes caused by the divacany complex. Further evidence for an independent origin of the barrier increase is provided by the

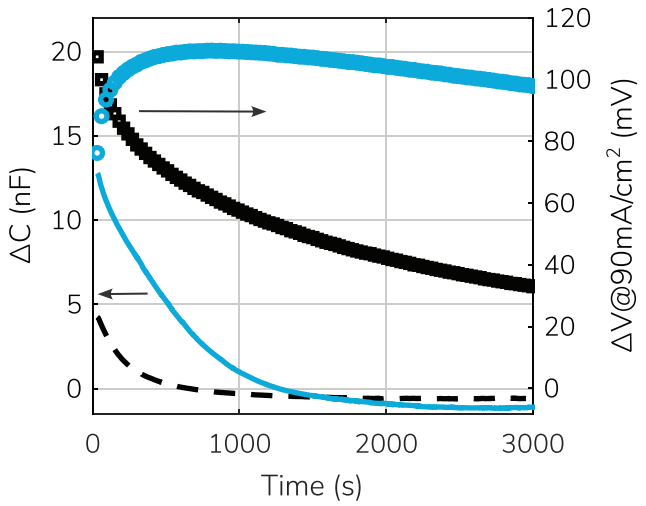


**Fig. 7.** Relaxation of the reverse-bias-induced metastable changes of the capacitance (lines, left vertical axis) and of the IV shift (symbols, right vertical axis) after continuous (blue) and intermittent (black) reverse-bias treatments of 600 s.

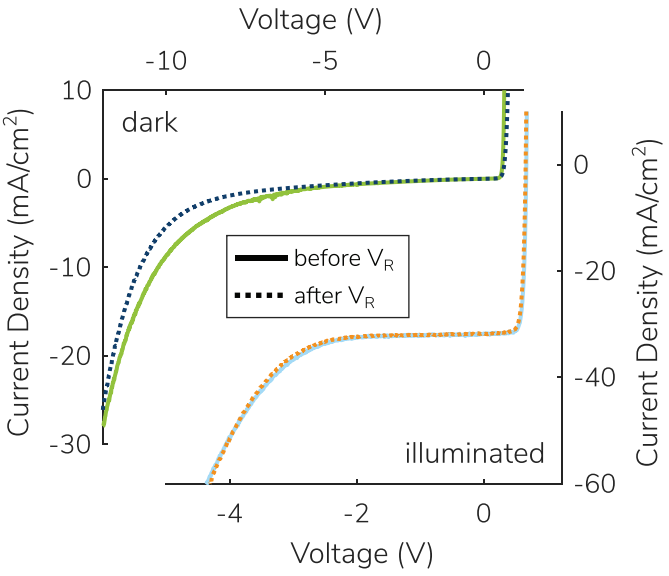


**Fig. 8.** Influence of a reverse-bias treatment (continuous −5 V for 10 min in the dark) on the dark (left and top axis) and illuminated (right and bottom axis) reverse IV characteristics.

relaxation behaviour of the reverse-bias-induced changes which is given in Figure 7: The time scales of the relaxation indicate that the processes for the IV shift and the capacitance shift are different.

An alternative origin of the barrier increase due to reverse bias has been proposed by Vidal Lobarda et al. [34], who were able to model the IV shift by an increased valence band barrier at the CIGS/Mo back interface due to a reduced absorber doping. In principle, such a process could be caused by migration of positive ions (such as Cu) which would be driven towards the back interface by the electric field under reverse bias [35] and would lead to a reduction of the net doping. With increasing duration of the $V_R$ treatment the low-doping region would spread further towards the front of the absorber. Once it reaches the main space-charge region it would lead to a decrease in the measured capacitance which agrees well with our results in Figure 6c+d.

Although the two proposed mechanisms for the reverse-bias metastability operate at different ends of the absorber layer, the relaxation results in Figure 7 reveal a certain amount of interaction: After the continuous $V_R$ treatment the IV shift does not start to actually decrease before the capacitance has relaxed completely. Possibly, the increased positive charge at the front interface due to the divacancy complex transition facilitates the migration of the positive ions towards the back interface. This effect is not observed for the intermittent $V_R$ treatment where the charge redistribution is much smaller.

The results in Figure 6 have shown that noticeable changes of the cell properties already occur after 60 s of continuous reverse-bias treatment. When measuring a typical reverse IV curve, the cell is usually at a negative voltage for a similar period of time. Therefore, the reverse IV curve may be influenced by metastable changes that are caused by measuring it. In the final part of this section, we thus try to assess the effects of a reverse-bias treatment on the reverse IV characteristics.

For this purpose we applied a voltage of $V_R = -5$ V continuously for 600 s in the dark as above, and measured the reverse IV curve before and after this treatment using intermittent voltage sweeps (in order to suppress measurement-induced heating effects). In some samples the effect on the *illuminated* reverse characteristics under standard test conditions (STC) was tested, and in other samples the effect on the *dark* IV was tested. Exemplary results are shown in Figure 8. It is apparent, that there is a systematic difference between the IV curves before (solid lines) and after (dotted lines) the $V_R$ treatment, but this difference is rather small: In terms of breakdown voltage, the $V_R$ treatment leads to an increase of the breakdown voltage in the range of a few tens of mV for the IV under illumination and of about 0.6 V for the dark IV. Performing analyses for Fowler-Nordheim and Poole-Frenkel tunneling as in Section 3 reveals that the reason for this slight increase in breakdown voltage seems to be an increase in the associated tunneling barriers: For the reverse IV under illumination $\Phi_{FN}$ rises by about 10% and $\Phi_{PF}$ by 1/3 on average; and for the reverse IV in the dark $\Phi_{FN}$ rises by about 30% and here a voltage region dominated by the Poole-Frenkel mechanism could not be identified.

As a conclusion, the effects induced by metastable changes during the measurement of a reverse IV curve are rather small and probably negligible in most cases. Nevertheless, using intermittent voltage sweeps for a reverse IV measurement will reduce any metastabilities and their distortions even further.

## 5 Conclusions

The approach of intermittent voltage application during reverse-bias measurements has been shown to reduce the measurement-induced heating of the device to a negligible amount. This opens up new opportunities to investigate the cell physics at negative voltages: Firstly, it allows for obtaining reverse-bias characteristics in which the device temperature can be assumed to be constant. This makes it easier to compare experimental results with models and simulations that do not incorporate thermal physics. Secondly, the comparison of results from intermittent and continuous voltage application may be used to study temperature effects of reverse-bias characteristics. In this way we were able to show that the reverse breakdown is mainly shifted towards lower absolute voltages by the measurement-induced heating, but that the tunneling nature of the breakdown does not change. Further, the dynamics of the reverse-bias-induced metastability are basically slowed down when using the intermittent measurement approach. However, the different rates of the metastable changes in space-charge capacitance and transport barrier suggested that in addition to the charge redistribution near the front interface (Lany-Zunger model), a charge redistribution at the back interface may take place, possibly as a result of ion migration.

The authors would like to thank the NICE Solar Energy GmbH for providing the samples and Abdel Kader Ndoukoue Chintouo for helping with the metastability measurements. We gratefully acknowledge funding by the German Ministry of Economic Affairs and Climate Action under grants "optiCIGS" (number 0325724F) and "optiCIGS-II" (number 0324297F).

## Author contribution statement

SJH devised the metastability part of the manuscript, did measurements and data analysis, and wrote the manuscript. AK did measurements and data analysis for the metastability part of the manuscript. MR devised and supervised the measurements of the first part of the manuscript. BP and AG contributed ideas on how to measure the "true" reverse IV curve. JN did measurements and data analysis for the first part of the manuscript, and reviewed and edited the manuscript.

## References

1. T.J. Silverman et al., IEEE J. Photovolt. **5**, 1742 (2015)
2. M. Nardone et al., Sol. Energy **139**, 381 (2016)
3. E. Palmiotti et al., Sol. Energy **161**, 1 (2018)
4. H. Guthrey et al., IEEE J. Photovolt. **8**, 1833 (2018)
5. P. Szaniawski et al., Thin Solid Films **535**, 326 (2013)
6. K. Bakker et al., IEEE J. Photovolt. **12**, 1412 (2022)
7. M. Igalson et al., Thin Solid Films **480**, 322 (2005)
8. A. Urbaniak et al., MRS Online Proceedings Library **1012**, 1216 (2007)
9. A. Urbaniak et al., J. Appl. Phys. **106**, 063720 (2009)
10. M. Igalson et al., Sol. Energy Mater. Sol. Cells **93**, 1290 (2009)
11. M. Igalson et al., in *25th EUPVSEC / 5th World Conference on Photovoltaic Energy Conversion*, (2010), pp. 3436–3441
12. T. Ott et al., in *26th EUPVSEC* (2011), pp. 2421–2424
13. S. Siebentritt et al., Prog. Photovolt: Res. Appl. **18**, 390 (2010)
14. S. Lany et al., J. Appl. Phys. **100**, 113725 (2006)
15. S. Puttnins et al., Sol. Energ. Mat. Sol. Cells **120**, 506 (2014)
16. P. Szaniawski et al., IEEE J. Photovolt. **7**, 1136 (2017)
17. R.H. Fowler et al., Proc. Royal Soc. A **119**, 173 (1928)
18. J. Frenkel, Phys. Rev. **54**, 647 (1938)
19. S. Puttnins et al., in *Proceedings of the 26th EUPVSEC* (2014), pp. 2432–2434
20. J. Neerken et al., EPJ Photovolt. **13**, 26 (2022)
21. G. Pananakakis et al., J. Appl. Phys. **78**, 2635 (1995)
22. A.K. Agarwal et al., IEEE Electr. Dev. Lett. **18**, 592 (1997)
23. C. Frisk et al., J. Phys. D: Appl. Phys. **47**, 485104 (2014)
24. S. Dongaonkar et al., IEEE Electron Device Lett. **31**, 1266 (2010)
25. A. Zelenina et al., Appl. Phys. Lett. **111**, 213903 (2017)
26. R. Herberholz et al., Eur. Phys. J. Appl. Phys. **6**, 131 (1999)
27. M. Igalson et al., MRS Online Proceedings Library **668**, 92 (2000)
28. P. Zabierowski et al., Thin Solid Films **387**, 147 (2001)
29. M. Igalson et al., Thin Solid Films **431–432**, 153 (2003)
30. A. Urbaniak et al., MRS Online Proceedings Library **1165**, 108 (2009)
31. A. Urbaniak et al., Thin Solid Films **517**, 2231 (2009)
32. S. Dongaonkar et al., in *2012 38th IEEE Photovoltaic Specialists Conference* (IEEE, 2012), pp. 000868–000872
33. M. Igalson et al., Sol. Energ. Mat. Sol. Cells **80**, 195 (2003)
34. R.V. Lorbada et al., Energies **13**, 4753 (2020)
35. J.F. Guillemoles et al., J. Phys. Chem. B **104**, 4849 (2000)

**Cite this article as**: Stephan J. Heise, Asliddin Komilov, Michael Richter, Bart Pieters, Andreas Gerber, Janet Neerken, Reverse-bias behaviour of thin-film solar cells: effects of measurement-induced heating, EPJ Photovoltaics **14**, 17 (2023)